Available online at www.sciencedirect.com

ScienceDirect

Nuclear Physics B 960 (2020) 115208

NUCLEAR PHYSICS B

www.elsevier.com/locate/nuclphysb

Constraints on the quark mixing matrix with vector-like quarks

Drona Vatsyayan, Anirban Kundu *

Department of Physics, University of Calcutta, 92 Acharya Prafulla Chandra Road, Kolkata 700009, India

Received 12 July 2020; received in revised form 10 September 2020; accepted 3 October 2020
Available online 6 October 2020
Editor: Hong-Jian He

Abstract

While a chiral fourth generation of quarks is almost ruled out from the data on Higgs boson production and decay at the Large Hadron Collider, vector-like quarks are still a feasible option to extend the fermionic sector of the Standard Model. Such an extension does not suffer from any anomalies and easily passes the constraints coming from oblique electroweak parameters. We consider such minimal extensions with $SU(2)$ singlet and doublet vector-like quarks that may mix with one, or at the most two, of the Standard Model quarks. Constraints on the new mixing angles and phases are obtained from several $\Delta B = 1$ and $\Delta B = 2$ processes.

1. Introduction

While all flavour observables, both CP-conserving and CP-violating, are more or less well explained by the 3×3 Cabibbo-Kobayashi-Maskawa (CKM) matrix, it is pertinent to investigate whether one can still accommodate one or more extra quarks. The new quarks can be chiral, like their Standard Model (SM) counterparts, or vector-like, where both left- and right-chiral components transform identically under the $SU(2)$ of weak interaction. A chiral fourth generation [1,2] that gets its mass through the same Higgs mechanism as the other three generations do, is more or less ruled out from the induced oblique corrections [3] and the data on Higgs boson

* Corresponding author.
E-mail addresses: dronavatsyayan@gmail.com (D. Vatsyayan), anirban.kundu.cu@gmail.com (A. Kundu).

https://doi.org/10.1016/j.nuclphysb.2020.115208

production and decay at the Large Hadron Collider (LHC) [4–7], unless the scalar sector of the Standard Model (SM) is extended [8]. However, vector-like quarks (VQ) easily evade such a constraint [9]. Moreover, by construction, inclusion of VQs still keeps the SM free from any gauge or mixed anomalies.

The VQs appear naturally in many extensions of the SM, and their effects and signatures have been thoroughly investigated. An overview of the phenomenology and searches for heavy VQs has been provided in Ref. [10]. For example, the $SU(2)$ doublet VQs in the topflavour seesaw models, and their signatures at the LHC, have been discussed in Refs. [11,12], or the role of the VQs in Higgs inflationary scenarios in Ref. [13]. For the study of nonunitarity of the CKM matrix, or the implications of a singlet down-type VQ, and its implications at the LHC, we refer the reader to Refs. [14–17]. The radiative decays of the b-hadrons were discussed in Refs. [18–20], while the role of VQs in B_s - $\overline{B_s}$ mixing was investigated in Refs. [21–24], and that in semileptonic and hadronic B-decays in Ref. [25].

In this work, we would be interested to find out how much mixing any new VQ may have with the SM quarks. For simplicity, we consider only one charge $+\frac{2}{3}$ VQ, called t', and/or only one charge $-\frac{1}{3}$ VQ, called b'. (Thus, SM gauge singlet VQs, a possible fermionic dark matter candidate, are outside our purview.) In other words, we would like to extend the CKM matrix by a row, or a column, or both, and try to find the bound on the new elements. Such studies have been performed earlier [22,26–29], and we will build on those studies, armed with more precise experimental data. Our main tool will be the loop-mediated $\Delta B = 1$ ($b \to s\gamma$, $B_s \to \mu^+\mu^-$) or $\Delta B = 2$ (B_s - $\overline{B_s}$ mixing) processes, and occasionally, the decay $Z \to b\overline{b}$. This is one of the reasons why we will not discuss the chiral fourth generation with more scalar fields, as those scalars affect these observables in a nontrivial way. A good example is the radiative b decay, $b \to s\gamma$, which is affected by the charged scalar loop. Thus, the bounds on the new CKM elements are meaningful only if we have a complete control over the parameters of the scalar potential. As a spin-off, we will also show how anomalous top decays like $t \to c\gamma$ and $t \to cZ$ are affected.

If a chiral quark is extremely massive, say of the order of a TeV, the Yukawa coupling will be badly nonperturbative, and no loop calculations are trustworthy [30]. For VQs, one does not face such a problem, as they can have a mass term without symmetry breaking. No such heavy quarks have been observed, so for our analysis, we will keep their masses fixed at 2 TeV. This is just outside the LHC reach; however, in future, only the luminosity of LHC, and not the energy reach, will increase, so anything beyond 2 TeV should remain undiscovered. This increases the importance of such indirect detection studies.

The paper is organised as follows. In Section 2, we provide a short introduction to the VQ models as well as a brief summary of the SM expressions for various loop-mediated observables that are relevant for our study. We also enlist the data that will be used in our analysis. In Section 3, we recast these expressions in the framework of the extended SM with vector-like singlet or doublet quarks. In Section 4, we display our results for each of these models, followed by the summary and conclusion in Section 5.

2. The toolbox

The charged current Lagrangian in the SM involving the stationary quark fields looks like

$$\mathcal{L}_{cc} = -\frac{g}{\sqrt{2}}\,\overline{u}_i V_{ij}\gamma^\mu P_L d_j W^+_\mu + \text{h.c.} \tag{1}$$

Table 1
Magnitudes of the directly measured CKM matrix elements, taken from Ref. [31].

Element	Value	Element	Value	Element	Value
V_{ud}	0.97370 ± 0.00014	V_{us}	0.2245 ± 0.0008	V_{ub}	$(3.82 \pm 0.24) \times 10^{-3}$
V_{cd}	0.221 ± 0.004	V_{cs}	0.987 ± 0.011	V_{cb}	$(41.0 \pm 1.4) \times 10^{-3}$
				V_{tb}	1.013 ± 0.030

where $i, j = 1, 2, 3$ are the generation indices, $P_L = \frac{1}{2}(1 - \gamma_5)$, and V is the CKM matrix. By construction, V is unitary, and the magnitudes of seven of the elements, as determined from tree-level processes, are as follows:

The elements V_{td} and V_{ts} can only be determined from B^0 - $\overline{B}^0$ or B_s - $\overline{B_s}$ mass difference, or indirectly from the unitarity of the CKM matrix. In our analysis, we will implicitly assume that the seven CKM elements shown in Table 1 are not affected in any significant way by the VQs. In particular, we will strictly assume that the mixing of the VQs with the first generation vanishes, so that processes like K-decays remain unaffected.

2.1. Introducing the vector-like quarks

Let us first introduce a charge $-\frac{1}{3}$ VQ, b', which is an $SU(2)$ singlet. The charged current Lagrangian now reads

$$\mathcal{L}_{cc} = -\frac{g}{\sqrt{2}} \overline{u}_i \mathcal{U}^{\dagger}_{ij} \mathcal{D}_{jk} \gamma^{\mu} P_L d_k W^{+}_{\mu} + \text{h.c.} \tag{2}$$

where $\mathcal{U}$ and $\mathcal{D}$ are the 3×3 and 4×4 basis transformation matrices. The indices can have the following values: $i, j = 1, 2, 3$, and $k = 1, 2, 3, 4$. Hence, the CKM matrix $V \equiv \mathcal{U}^{\dagger}\mathcal{D}$ is a 3×4 matrix. Obviously, the SM part of V is no longer unitary, and we cannot use the unitarity condition to constrain its elements. The following points immediately become evident:

- Such a 3×4 CKM matrix can be parametrized by 9 independent parameters, including 6 real angles and 3 phases. To see this, let us take $\mathcal{U} = \mathbf{1}$, the identity matrix, so that V is just the top 3×4 block of $\mathcal{D}$. The row unitarity conditions still hold, which gives 9 constraints, and one can remove 6 irrelevant phases through quark phase redefinition. Thus, one is left with $2 \times 12 - 9 - 6 = 9$ independent parameters.
- The tree-level Z-mediated flavour-changing neutral current (FCNC) processes will be present in the down sector, but not in the up sector. The vertex factor for $\overline{d}_{iL} d_{jL} Z$ tree-level interaction is

$$g^{Z}_{ijL} = \frac{g}{c_W} \left(-\frac{1}{2} + \frac{1}{3} s^2_W \right) \delta_{ij} + \frac{g}{2c_W} \mathcal{D}^{*}_{4i} \mathcal{D}_{4j} \,, \tag{3}$$

  while there is no such FCNC for the right-chiral quarks (the situation is exactly the opposite for vector-like doublet quarks). We use the standard abbreviation of $s_W \equiv \sin\theta_W$, $c_W \equiv \cos\theta_W$. Such FCNC vertices can have important implications in flavour physics, and we may refer the reader to, *e.g.*, Refs. [32,33], for its effects to the CP asymmetries in the B^0 - $\overline{B}^0$ system.
- Only if we consider the texture where $\mathcal{U} = \mathbf{1}$ and hence $\mathcal{D}_{3\times4} = V$, the FCNC vertex factor in Eq. (3) can be written as

$$g^Z_{ijL}\ (i \neq j) = -\frac{g}{2c_W}\left[V^*_{ui}V_{uj} + V^*_{ci}V_{cj} + V^*_{ti}V_{tj}\right], \tag{4}$$

which can potentially be most significant for the bsZ vertex.

- Again, under such assumptions like $\mathcal{U} = \mathbf{1}$, the 3×4 CKM matrix is a part of the full 4×4 $\mathcal{D}$ matrix, which is unitary, and we can use the row unitarity conditions as constraints, *e.g.*,

$$\sum_{i=d,s,b,b'} |V_{ti}|^2 = 1\,. \tag{5}$$

Similarly, one can introduce a charge $+\frac{2}{3}$ singlet VQ, t', for which the CKM matrix V is 4×3. The FCNC will be present only for left-chiral up-type quarks, parametrized by a vertex factor analogous to that in Eq. (3),

$$g^Z_{ijL} = \frac{g}{c_W}\left(\frac{1}{2} - \frac{2}{3}s^2_W\right)\delta_{ij} - \frac{g}{2c_W}\mathcal{U}^*_{4i}\mathcal{U}_{4j}\,, \tag{6}$$

which leads to the tree-level top FCNC decays like $t \to cZ$.

We will consider the following simplified models for singlet VQ (not all of them can be constrained from flavour observables):

1. **Model VQ-S-D1**: A charge $-\frac{1}{3}$ VQ b' with $V_{ub'} = V_{cb'} = 0$, $V_{tb'} \neq 0$. The structure forbids any tree-level FCNC. However, there will be new one-loop contributions to ZWW and γWW vertices, as well as to $t\bar{t}$ production.[1] As we will show, this model remains essentially unconstrained, except the bound on $|V_{tb'}|$ coming from unitarity, see Eq. (5).
2. **Model VQ-S-D2**: Similar to VQ-S-D1, except that both $V_{tb'}$ and $V_{cb'}$ are taken to be nonzero, while $V_{ub'}$ is kept fixed at zero. One of these two new elements can contain a nontrivial phase. The tree-level bsZ interaction contributes to B_s - $\overline{B_s}$ mixing, $b \to s\gamma$, and $B_s \to \mu^+\mu^-$. There will also be loop-mediated contributions to $t \to c\gamma$ [34]. To maximise the effects of the VQs, we will take $\mathcal{U} = \mathbf{1}$, so that the FCNC coupling is given by Eq. (4).
3. **Model VQ-S-U1**: A mirror image of VQ-S-D1, with one singlet charge $+\frac{2}{3}$ quark t', and $V_{t'd} = V_{t's} = 0$ while $V_{t'b} \neq 0$. The CKM matrix is 4×3. The texture affects the triple gauge vertices at one-loop, as well as the decay $Z \to b\bar{b}$. Again, the most significant constraint on $V_{t'b}$ comes from the column unitarity, analogous to Eq. (5), under possible assumptions about $\mathcal{D}$.
4. **Model VQ-S-U2**: Again, similar to VQ-S-U1, but keeping two nonzero mixing elements $V_{t'b}$ and $V_{t's}$. The same observables as for VQ-S-D2 are affected, but there is a major difference. For VQ-S-D2, processes like B_s - $\overline{B_s}$ mixing were affected by the tree-level bsZ vertex, while $t \to c\gamma$ was affected by one-loop processes (with the b' quark running in the loop). For VQ-S-U2, it is just the opposite: $t \to c\gamma$ is affected by the tree-level tcZ interaction, while B-physics observables are affected by one-loop processes. For the VQ-S-U type models, we will consider $\mathcal{U}_{3\times4} = V^\dagger$ and $\mathcal{D} = \mathbf{1}$; this maximises the FCNC effects.

Next, let us consider a degenerate (so that constraints from oblique parameters [9] are under control) vector-like doublet $Q = (t' \quad b')^T$, for which both left- and right-chiral components are in the fundamental representation of weak $SU(2)$. Eq. (2) now extends to all the left-chiral quarks, *i.e.*, all the indices i, j, k run from 1 to 4. Obviously, there is no tree-level FCNC in

[1] The letters S and D in the model denote that the VQ is singlet and down-type.

the left-chiral sector. In the right-chiral sector, the FCNC vertices, for the up- and down-quark sectors respectively, are

$$g^{uZ}_{ijR}\ (i \neq j) = \frac{g}{2c_W}\ (\mathcal{U}_R)^*_{4i}\ (\mathcal{U}_R)_{4j}\ ,$$
$$g^{dZ}_{ijR}\ (i \neq j) = -\frac{g}{2c_W}\ (\mathcal{D}_R)^*_{4i}\ (\mathcal{D}_R)_{4j}\ , \tag{7}$$

where $\mathcal{U}_R$ and $\mathcal{D}_R$ are the basis transformation matrices for the right-chiral up- and down-type quarks respectively. The flavour-conserving vertices are exactly like the SM. As the CKM matrix does not contain any information about $\mathcal{U}_R$ or $\mathcal{D}_R$ matrices, one may either treat them as free parameters, or just set all the off-diagonal terms to zero (*i.e.*, $\mathcal{U}_R = \mathcal{D}_R = \mathbf{1}$).

One may note that the 4×4 CKM matrix is unitary, so it may be parametrized by 6 real angles and 3 complex phases. We do not need to know the individual $\mathcal{D}_L$ or $\mathcal{U}_L$ matrices, and the analysis is similar to that for a sequential fourth generation [26]. The unitarity constraints can now be invoked, *e.g.*,

$$|V_{t'b}|^2 = 1 - \sum_{i=u,c,t} |V_{ib}|^2\ . \tag{8}$$

We will take $\mathcal{U}_R = \mathcal{D}_R = \mathbf{1}$, so that for doublet VQ, we only need to consider the loop-driven processes. Two models will be discussed, namely:

1. **Model VQ-D-U2**: Apart from $V_{t'b'}$, only two other elements involving a VQ are taken to be nonzero: $V_{t's}$ and $V_{t'b}$. The b' quark decays through a real (if kinematically allowed) or a virtual t'. This texture affects processes like B_s - $\overline{B_s}$ mixing, $b \to s\gamma$, $B_s \to \mu^+\mu^-$, and $Z \to b\overline{b}$. Another variant is to take $V_{t'd} \neq 0$ and $V_{t's} = 0$; all the above processes are, in that case, replaced by their $s \to d$ analogues.
2. **Model VQ-D-D2**: The nonzero elements are taken to be $V_{cb'}$ and $V_{tb'}$, apart from $V_{t'b'}$. Such a choice affects top pair production, and decays like $t \to c\gamma$.

One might be wondering about the constraints coming from the oblique parameters. We refer the reader to the comprehensive analysis done in Ref. [9]. This contains the most general case of an arbitrary number of singlet and doublet VQs, as well as the specific cases of a down-type or up-type singlet VQ. It turns out that for small mixing with chiral quarks (at the level that we are considering), all the models fall safely within the allowed regions of the oblique parameters.

Being loop-driven in the SM, the amplitudes for all the processes that we consider can be written in a generic way:

$$\mathcal{M} = \sum_i A_i \mathcal{V}_i\ F_i^{IL}(m)\,, \tag{9}$$

where i runs over all the individual amplitudes, including higher order QCD and electroweak corrections, $\mathcal{V}_i$ is some combination of the CKM elements, and $F_i^{IL}(m)$ is the relevant Inami-Lim function, which depends on the quark (mostly top) and the gauge boson masses. All the other constants are clubbed in A_i. For our analysis, we will take only the leading order effects coming from the VQs and try to find out the allowed region of the CKM elements vis-à-vis the VQ couplings.

Table 2
Values of the parameters required for determination of $|V_{ts}|$. The error bars are at 2σ [31].

Parameter	Value	Parameter	Value
G_F	1.1663787×10^{-5} GeV^{-2}	η_B	0.55 ± 0.02
M_W	80.379 ± 0.024 GeV	m_t	172.4 ± 1.4 GeV
M_{B_s}	5366.88 ± 0.28 MeV	ΔM_s	$(1.1683 \pm 0.0026) \times 10^{-8}$ MeV
$\sqrt{B_{B_s}} F_{B_s}$	274 ± 16 MeV		

2.2. $\Delta B = 2$ processes: B_q - $\overline{B_q}$ mixing

The mass difference ΔM_q $(q = d, s)$ for the B_q - $\overline{B_q}$ system is given by

$$\Delta M_q = \frac{G_F^2}{6\pi^2} \left|V_{tq} V_{tb}^*\right|^2 \eta_B M_{B_q} (B_{B_q} F_{B_q}^2) M_W^2 S_0(x_t) \,, \tag{10}$$

where $x_t = m_t^2/M_W^2$, and the Inami-Lim function is

$$S_0(x_t) = \frac{4x_t - 11x_t^2 + x_t^3}{4(1-x_t)^2} - \frac{3x_t^2 \log x_t}{2(1-x_t)^3} \,, \tag{11}$$

where we neglect the charm- and up-quark contributions. We will focus only on the $q = s$ case. All other relevant quantities are shown in Table 2.

This leads to

$$\begin{aligned} &x_t = 4.60 \pm 0.04 \,, \quad S_0(x_t) = 2.52 \pm 0.21 \,, \\ &\Delta M_s = (8.3 \pm 0.9) \times 10^{-6} \text{ MeV} \times |V_{ts}|^2 \end{aligned} \tag{12}$$

The phase coming from the mixing in the B_s - $\overline{B_s}$ system is given by

$$M_{12}^s = \frac{1}{2} \Delta M_s \, \exp(-2i\beta_s) \,, \tag{13}$$

where M_{12}^s is the absorptive part of the (12)-element of the Hamiltonian matrix, and the phase comes from V_{ts}^2, whose value is found to be [31]

$$\beta_s = (1.1 \pm 1.6) \times 10^{-2} \,. \tag{14}$$

2.3. $\Delta B = 1$ processes

2.3.1. $b \to s\gamma$

The radiative decay $b \to s\gamma$ has a branching ratio of [35]

$$\text{Br}(b \to s\gamma) = (3.32 \pm 0.15) \times 10^{-4} \,, \quad E_\gamma > 1.6 \text{ GeV} \tag{15}$$

with a corresponding SM prediction of [36,37][2]

$$\text{Br}(b \to s\gamma)_{\text{SM}} = (3.36 \pm 0.23) \times 10^{-4} \,, \quad E_\gamma > 1.6 \text{ GeV} \,. \tag{16}$$

To reduce the theoretical uncertainties, one generally uses the ratio of the decay rates:

[2] The SM uncertainties may have been underestimated by about a factor of two, which provides more room for VQs and/or any other new physics [38].

Table 3
Values of different parameters required for evaluating $\Delta B = 1$ processes taken from Ref. [31], and F_{B_s} from Ref. [40].

Parameter	Value	Parameter	Value
$\alpha(M_Z)$	1/129	m_b	4.18 GeV
$\alpha_s(M_Z)$	0.1179	M_Z	91.1876 GeV
s_W^2	0.231	m_μ	105.6584 MeV
$\tau_{B_{sH}}$	1.620 ps	F_{B_s}	230.3 ± 1.3 MeV

$$R \equiv \frac{\Gamma(B \to X_s\gamma)}{\Gamma(B \to X_c e\overline{\nu}_e)} \simeq \frac{\Gamma(b \to s\gamma)}{\Gamma(b \to ce\overline{\nu}_e)}\,. \tag{17}$$

At leading logarithmic order, the ratio can be written as

$$R = \frac{|V_{ts}^* V_{tb}|^2}{|V_{cb}|^2}\,\frac{6\alpha}{\pi f(z)}\,\left|C_{7\gamma}^{(0)\text{eff}}(\mu)\right|^2\,, \tag{18}$$

where

$$f(z) = 1 - 8z^2 - 8z^6 - z^8 - 24z^4 \ln z; \quad z = \frac{m_c}{m_b} \tag{19}$$

is the phase space factor in semileptonic b-decays. The effective Wilson coefficient $C_{7\gamma}^{(0)\text{eff}}(\mu)$ is given by [39]

$$C_{7\gamma}^{(0)\text{eff}}(\mu) = \eta^{16/23} C_{7\gamma}^{(0)}(M_W) + \frac{8}{3}\left(\eta^{14/23} - \eta^{16/23}\right) C_{8G}^{(0)}(M_W) + C_2^{(0)}(M_W) \sum_{i=1}^{8} h_i \eta^{a_i}\,, \tag{20}$$

where

$$\eta = \frac{\alpha_s(M_W)}{\alpha_s(\mu)}\,. \tag{21}$$

The values of $C_2^{(0)}(M_W) \sim 1$, a_i and h_i can be found in Ref. [39]. $C_{7\gamma}^{(0)}(M_W)$ and $C_{8G}^{(0)}(M_W)$ are expressed in terms of the Inami-Lim functions $D_0'(x_t)$ and $E_0'(x_t)$ respectively with $x_t = m_t^2/M_W^2$:

$$C_{7\gamma}^{(0)}(M_W) = -\frac{1}{2} D_0'(x_t) \equiv \frac{3x_t^3 - 2x_t^2}{4(x_t-1)^4} \log x_t + \frac{-8x_t^3 - 5x_t^2 + 7x_t}{24(x_t-1)^3} \tag{22}$$

$$C_{8G}^{(0)}(M_W) = -\frac{1}{2} E_0'(x_t) \equiv \frac{-3x_t^2}{4(x_t-1)^4} \log x_t + \frac{-x_t^3 + 5x_t^2 + 2x_t}{8(x_t-1)^3} \tag{23}$$

The other parameters entering in Eq. (20) are given in Table 3. A similar analysis follows for $b \to d\gamma$, with the suitable replacement of $s \to d$.

2.3.2. $B_s \to \mu^+\mu^-$

The branching ratio for $B_s \to \mu^+\mu^-$ is [31]

$$\text{Br}(B_s \to \mu^+\mu^-) = (3.0 \pm 0.4) \times 10^{-9}\,, \tag{24}$$

whereas the SM prediction is [41,42]

$$\text{Br}(B_s \to \mu^+\mu^-)_{\text{SM}} = (3.65 \pm 0.23) \times 10^{-9}\,. \tag{25}$$

The expression for the branching ratio is given by

$$\mathrm{Br}(B_s \to \mu^+\mu^-) = \tau_{B_{sH}} \frac{G_F^2}{\pi} \left(\frac{\alpha}{2\pi s_W^2}\right)^2 F_{B_s}^2 m_\mu^2 M_{B_s} \sqrt{1-4\frac{m_\mu^2}{M_{B_s}^2}} \left|V_{tb}^* V_{ts}\right|^2 |C_A(\mu_b)|^2 , \tag{26}$$

where $\tau_{B_{sH}}$ is the lifetime of the heavier B_s eigenstate.[3] The Wilson coefficient C_A, evaluated at the regularisation scale μ_b, gets contribution from both W-mediated box and Z-mediated penguin amplitudes:

$$C_A = C_{A,W} + C_{A,Z} , \tag{27}$$

and each of the C_As can be written as

$$C_{A,W(Z)} = \sum_{n=0}^{\infty} C_{A,W(Z)}^{(n)} \left(\frac{\alpha_s}{4\pi}\right)^n , \tag{28}$$

indicating the leading order (LO) terms and the higher-order QCD corrections; results up to $n = 2$ can be found in Ref. [42]. The LO contribution is given by the Inami-Lim function

$$C_A^{(0)} = \frac{x_t}{16}\left[\frac{x_t-4}{x_t-1} + \frac{3x_t}{(x_t-1)^2}\log x_t\right] . \tag{29}$$

The higher-order contributions can be parametrized by

$$C_A(\mu_b) = \eta_Y C_A^{(0)} , \tag{30}$$

with $\eta_Y = 0.905$.

2.4. Other loop-induced processes

2.4.1. $t \to c\gamma$

The partial decay width for the radiative decay $t \to c\gamma$ is given by

$$\Gamma(t \to c\gamma) = \frac{1}{\pi}\left[\frac{m_t^2 - m_c^2}{2m_t}\right]^3 \left(\left|A_\gamma\right|^2 + \left|B_\gamma\right|^2\right) , \tag{31}$$

where A_γ and B_γ are respectively the vector and axial form factors, whose expressions may be found in Ref. [34]. The three-point Passarino-Veltman C-functions involved in the form factors are numerically evaluated with LoopTools [43]. The SM prediction for $\mathrm{Br}(t \to c\gamma)$ is approximately 4×10^{-14}.

2.4.2. $t \to cZ$

In the SM, the partial decay width for $t \to cZ$ is given by [44]:

$$\Gamma(t \to cZ) = \Gamma(t \to c\gamma) + \frac{\lambda^{1/2}(1,\, M_Z^2/m_t^2,\, m_c^2/m_t^2)}{16\pi\, m_t M_Z^2}\,\mathcal{F} , \tag{32}$$

[3] For B^0, one can just use the average of the lifetimes of the two neutral mass eigenstates. The width difference is non-negligible for B_s.

Table 4
Effect of vector-like quarks on some flavour observables. Only for VQ-S-U2, $t \to cZ$ occurs at the tree-level, with our ansatz for the texture of the quark mixing matrices.

Model	B_s - $\overline{B_s}$	$b \to s\gamma$	$B_s \to \mu^+\mu^-$	$t \to c\gamma$	$t \to cZ$	$Z \to b\overline{b}$
VQ-S-D1	—	—	—	—	—	—
VQ-S-D2	√	√	√	√	√	—
VQ-S-U1	—	—	—	—	—	√
VQ-S-U2	√	√	√	√	√	√
VQ-D-U2	√	√	√	—	—	√
VQ-D-D2	—	—	—	√	√	—

where $\lambda(a,b,c) = a^2 + b^2 + c^2 - 2(ab + bc + ac)$, and $\mathcal{F}$ contains the CKM factors and the momenta of the particles involved. The branching fraction for the decay in SM is of the order of $\sim 10^{-14}$.

2.4.3. $Z \to b\overline{b}$

The ratio R_b, defined as

$$R_b = \frac{\Gamma(Z \to b\overline{b})}{\Gamma(Z \to \text{hadrons})} = (1 + 2/R_s + 1/R_c + 1/R_u)^{-1} \tag{33}$$

with $R_q \equiv \Gamma(Z \to b\overline{b})/\Gamma(Z \to q\overline{q})$, involves two non-universal corrections, namely, δ^b_{tQCD}, an $\mathcal{O}(\alpha_s^2)$ correction originating from doublets with large mass splitting, and δ_b, that represents the additional contribution to the $Zb\overline{b}$ vertex due to non-zero top quark mass [45]:

$$\delta_b = 2\,\frac{v_b + a_b}{v_b^2 + a_b^2}\,\text{Re}\,\delta_{b\text{-vertex}}, \qquad \delta_{b\text{-vertex}} = 2\left(\frac{\alpha}{2\pi}\right)|V_{tb}|^2\,F(x_t) \tag{34}$$

with $x_t = (m_t/M_W)^2$ and

$$F(x_t) = \frac{1}{8s_W^2}\left[x_t + 2.880\log x_t - 6.716 + \frac{1}{x_t}(8.368\log x_t - 3.408) + \frac{1}{x_t^2}(9.126\log x_t + 2.260) + \frac{1}{x_t^3}(4.043\log x_t + 7.410) + \ldots\right]. \tag{35}$$

Using the expressions given in Ref. [45] for R_c, R_s, R_u and δ^b_{tQCD}, one gets $R_b \approx 0.217$.

3. Modifications with vector-like quarks

With singlet or doublet VQs introduced, the processes discussed above get modified. Table 4 provides a quick display, which we elaborate in this Section. The model VQ-S-D1 cannot be constrained from any of these observables, except the row unitarity shown in Eq. (5). This, in conjunction with the fact that ΔM_d and ΔM_s are not affected by the VQ so that the SM estimates for $|V_{td}|$ and $|V_{ts}|$ are still valid, leads to a tiny value of $|V_{tb'}|$.

3.1. VQ-S-D2

3.1.1. B_s - $\overline{B_s}$ mixing

Due to the presence of a new vector-like down type singlet mixing with two generations, Eq. (10) now reads [21,22]

$$\Delta M_s = \frac{G_F^2}{6\pi^2}\,\eta_B M_{B_s}\left(B_{B_s}F_{B_s}^2\right) M_W^2\Bigg[\left|V_{ts}V_{tb}^*\right|^2 S_0(x_t) - 8\left|X_{sb}V_{ts}V_{tb}^*\right| Y_0(x_t) + \frac{4\pi s_W^2}{\alpha}\,\frac{\eta_Z^{B_s}}{\eta_B}\,|X_{sb}|^2\Bigg], \tag{36}$$

with

$$X_{ij} = \sum_{r=u,c,t} V_{ri}^* V_{rj} \tag{37}$$

and

$$Y_0(x_t) = \frac{x_t}{8}\left[\frac{x_t-4}{x_t-1} + \frac{3x_t}{(x_t-1)^2}\log x_t\right]. \tag{38}$$

In Eq. (36), the first term inside the parenthesis gives the SM box contribution, the second term comes from the amplitude with a tree-level FCNC coupling on one side and the SM loop on the other, while the last term is a pure Z-mediated tree-level FCNC contribution. We neglect the contributions due to charm and up quarks, and take $\eta_Z^{B_s} = 0.57$ [22].

3.1.2. $b \to s\gamma$

With a charge $-\frac{1}{3}$ VQ b' introducing FCNC couplings in the down-quark sector, the radiative decay $b \to s\gamma$ involves more penguin amplitudes, where the canonical W-propagator is replaced by either the Z boson, or the Higgs boson h [18]. The additional contributions to the Wilson coefficients $C_{7\gamma}$ and C_{8G} in Eqs. (22) and (23) are given by

$$\begin{aligned}
\delta C_{7\gamma}(M_W) &= \frac{X_{sb}}{V_{ts}^*V_{tb}}\left(\frac{23}{36} + \xi_s^Z + \xi_b^Z\right) + \frac{X_{sb'}X_{b'b}}{V_{ts}^*V_{tb}}\left[\xi_{b'}^Z(y_{b'}) + \xi_{b'}^h(w_{b'})\right], \\
\delta C_{8G}(M_W) &= \frac{X_{sb}}{V_{ts}^*V_{tb}}\left(\frac{1}{3} - 3\xi_s^Z - 3\xi_b^Z\right) - 3\frac{X_{sb'}X_{b'b}}{V_{ts}^*V_{tb}}\left[\xi_{b'}^Z(y_{b'}) + \xi_{b'}^h(w_{b'})\right],
\end{aligned} \tag{39}$$

where $X_{sb'}X_{b'b} \approx -X_{sb}$ (assuming $|\mathcal{D}_{44}|^2 \approx 1$), and

$$\begin{aligned}
\xi_s^Z &= \frac{1}{54}\left(-3 + 2s_W^2\right), \quad \xi_b^Z = \frac{1}{54}\left(-3 - 4s_W^2\right), \\
\xi_{b'}^Z(y_{b'}) &= -\frac{8 - 30y_{b'} + 9y_{b'}^2 - 5y_{b'}^3}{144(1-y_{b'})^3} + \frac{y_{b'}^2}{8(1-y_{b'})^4}\log y_{b'}, \\
\xi_{b'}^h(w_{b'}) &= -\frac{16w_{b'} - 29w_{b'}^2 + 7w_{b'}^3}{144(1-w_{b'})^3} + \frac{-2w_{b'} + 3w_{b'}^2}{24(1-w_{b'})^4}\log w_{b'},
\end{aligned} \tag{40}$$

with $y_i = (m_i/M_Z)^2$ and $(w_i = m_i/M_h)^2$ [18]. Three other Wilson coefficients, zero in the SM, receive non-zero contribution in this scenario:

$$C_3(M_W) = -\frac{1}{6}\frac{X_{sb}}{V_{ts}^*V_{tb}}, \quad C_7(M_W) = -\frac{2}{3}s_W^2\frac{X_{sb}}{V_{ts}^*V_{tb}}, \quad C_9(M_W) = \frac{2}{3}(1-s_W^2)\frac{X_{sb}}{V_{ts}^*V_{tb}}. \tag{41}$$

At the scale $\mu = 5$ GeV, one gets

$$\begin{aligned}
C_{7\gamma}^{(0)\text{eff}}(\mu) = &-0.158C_2(M_W) + 0.695C_{7\gamma}(M_W) + 0.085C_{8G}(M_W) \\
&+0.143C_3(M_W) + 0.101C_7(M_W) - 0.036C_9(M_W).
\end{aligned} \tag{42}$$

In the SM, $C_2(M_W) = 1$ because of the unitarity of the CKM matrix; here, it is better to use

$$C_2(M_W) = -\frac{V_{cs}^* V_{cb}}{V_{ts}^* V_{tb}}\,. \tag{43}$$

3.1.3. $B_s \to \mu^+\mu^-$

The contribution due to tree level Z exchange to Eq. (26) is given by [46]

$$\mathrm{Br}(B_s \to \mu^+\mu^-)_{\mathrm{VQ}} = \tau_{B_{sH}} \frac{G_F^2 F_{B_s}^2 M_{B_s} m_\mu^2}{8\pi} \sqrt{1 - \frac{4m_\mu^2}{M_{B_s}^2}} \left[\left(\frac{1}{2} - s_W^2\right)^2 + s_W^4\right] |X_{sb}|^2\,. \tag{44}$$

3.1.4. $t \to c\gamma$

The loop mediated contributions of b' to the form factors in Eq. (31) can be easily incorporated as

$$\delta A_\gamma = A_{\gamma,i}^{b'}, \quad \delta B_\gamma = B_{\gamma,i}^{b'} \tag{45}$$

where i indicates the contribution coming from various diagrams [34].

3.2. VQ-S-U1

With an additional up-type singlet quark t' and only $V_{t'b} \neq 0$, a similar constraint as for VQ-S-D1 comes from the column unitarity $\sum |V_{ib}|^2 = 1$. However, there is one decay channel where t' can affect. This is the modification of the $Zb\bar{b}$ vertex; the loop corrections due to t and t' modify the decay width $\Gamma(Z \to b\bar{b})$ and thus R_b. As all the effects due to large top quark mass are contained in the vertex correction factor δ_b, the mixing of top quark with vector quarks modifies the function F in Eq. (34), which is taken into account by making the substitution $F \to F + F_2$ [22,47], where

$$F_2(x_t) = \frac{1}{8s_W^2} \frac{Z_{tt} - 1}{2} x_t \left(2 - \frac{4}{x_t - 1} \log x_t\right)$$

and

$$Z_{ij} = \sum_{r=d,s,b} V_{ir}^* V_{jr}\,. \tag{46}$$

In addition to diagrams involving top quarks in the loop, there are triangle diagrams involving t's in the loop, or t and t'. Therefore, δ_b is modified as

$$\begin{aligned}\delta_{b\text{-vertex}} \approx \frac{\alpha}{\pi} \big(&|V_{tb}|^2 [F(x_t) + F_2(x_t)] + |V_{t'b}|^2 [F(x_{t'}) + F_2(x_{t'})] \\ &+ V_{tb}^* V_{t'b} (x_t, x_{t'}) F_3(x_t, x_{t'})\big)\,,\end{aligned} \tag{47}$$

where the t-t' contribution is given by the last term [22], with

$$\begin{aligned}F_3(x_t, x_{t'}) = \frac{1}{2s_W^2} \frac{\mathrm{Re} Z_{tt'}}{2} \Bigg[&- \frac{1}{x_t - x_{t'}} \left(\frac{x_{t'}^2}{x_{t'} - 1} \log x_{t'} - \frac{x_t^2}{x_t - 1} \log x_t\right) \\ &+ \frac{x_t x_{t'}}{x_{t'} - x_t} \left(\frac{x_{t'}}{x_{t'} - 1} \log x_{t'} - \frac{x_t}{x_t - 1} \log x_t\right)\Bigg]\,.\end{aligned} \tag{48}$$

Since, t' mixes only with third generation in this model, we have $Z_{tt'} = V_{tb}^* V_{t'b}$.

3.3. VQ-S-U2

3.3.1. B_s - $\overline{B_s}$ mixing

With the VQ t' in the loop, Eq. (10) is modified as

$$\Delta M_s = \frac{G_F^2}{6\pi^2} M_{B_s} (B_{B_s} F_{B_s}^2) M_W^2 \left[\eta_{tt} \left| V_{ts} V_{tb}^* \right|^2 S_0(x_t) + \eta_{t't'} \left| V_{t's} V_{t'b}^* \right|^2 S_0(x_{t'}) + 2\eta_{tt'} V_{ts} V_{tb}^* V_{t's} V_{t'b}^* \tilde{S}_0(x_t, x_{t'}) \right], \tag{49}$$

where

$$\tilde{S}_0(x_t, x_{t'}) = x_t \left[\log \frac{x_{t'}}{x_t} - \frac{3x_{t'}}{4(1-x_{t'})} - \frac{3x_{t'}^2 \log x_{t'}}{4(1-x_{t'}^2)} \right]. \tag{50}$$

In our analysis, we will take all QCD correction factors to be equal:

$$\eta_{tt} \approx \eta_{t't'} \approx \eta_{tt'} = \eta_B \,, \tag{51}$$

and neglect the contribution coming from the up and the charm quarks.

3.3.2. $b \to s\gamma$

Similarly, for the radiative decay with the t' quark loop, the additional contribution to the Wilson coefficients in Eqs. (22) and (23) can be written as

$$\begin{aligned} \delta C_{7\gamma}(M_W) &= -\frac{1}{2} \frac{V_{t's}^* V_{t'b}}{V_{ts}^* V_{tb}} D_0'(x_{t'}) \,, \\ \delta C_{8G}(M_W) &= -\frac{1}{2} \frac{V_{t's}^* V_{t'b}}{V_{ts}^* V_{tb}} E_0'(x_{t'}) \,, \end{aligned} \tag{52}$$

where

$$\begin{aligned} D_0'(x_{t'}) &= \frac{-8x_{t'}^3 - 5x_{t'}^2 + 7x_{t'}}{12(1-x_{t'})^3} + \frac{-3x_{t'}^3 + 2x_{t'}^2}{2(1-x_{t'})^4} \log x_{t'} \,, \\ E_0'(x_{t'}) &= \frac{-x_{t'}^3 + 5x_{t'}^2 + 2x_{t'}}{4(1-x_{t'})^3} + \frac{3x_{t'}^2}{2(1-x_{t'})^4} \log x_{t'} \,. \end{aligned} \tag{53}$$

3.3.3. $B_s \to \mu^+\mu^-$

In presence of t', the branching ratio for $B_s \to \mu^+\mu^-$ is given by

$$\mathrm{Br}(B_s \to \mu^+\mu^-) = \tau_{B_s H} \frac{G_F^2}{\pi} \left(\frac{\alpha}{4\pi s_W^2} \right) F_{B_s}^2 m_\mu^2 M_{B_s} \sqrt{1 - 4\frac{m_\mu^2}{M_{B_s}^2}}\, Y_m^2 \,, \tag{54}$$

where

$$Y_m = \eta_t V_{tb}^* V_{ts} Y_0(x_t) + \eta_{t'} V_{t'b}^* V_{t's} Y_0(x_t') \,. \tag{55}$$

Again, we use the approximation $\eta_t \approx \eta_{t'} = \eta_Y$ for our estimates.

3.3.4. $t \to c\gamma$

The introduction of t' induces new FCNC vertices in the up-quark sector. Thus, there will be new loop amplitudes with FCNC Z-vertices. The flavour diagonal couplings also get modified according to Eq. (6). The contribution of the new diagrams to the form factors in Eq. (31) is given in Ref. [34].

3.3.5. $t \to cZ$

Only in this class of models the FCNC decay $t \to cZ$ occurs at the tree-level, and its decay width, with next-to-leading order QCD corrections, can be written as

$$\Gamma(t \to cZ) = \frac{g^2}{128\pi\, c_W^2}\, |Z_{ct}|^2\, \frac{m_t^3}{M_Z^2} \left(1 - \frac{M_Z^2}{m_t^2}\right)^2 \left(1 + 2\frac{M_Z^2}{m_t^2}\right) \left[1 - \frac{2\alpha_s}{3\pi}\left(\frac{2\pi^2}{3} - \frac{5}{2}\right)\right], \tag{56}$$

where the charm quark mass has been neglected.

3.3.6. $Z \to b\overline{b}$

The contribution of the new singlet to the vertex correction factor for $Z \to b\overline{b}$ is described in Section 3.2. However, as t' mixes with two generations in this model, from Eq. (46) we have

$$Z_{tt'} = V_{ts}^* V_{t's} + V_{tb}^* V_{t'b}\,. \tag{57}$$

3.4. VQ-D-U2

In this model, the processes B_s - $\overline{B_s}$ mixing, $b \to s\gamma$ and $B_s \to \mu^+\mu^-$ receive an additional contribution from t' in the loop similar to the model VQ-S-U2, and the corresponding expressions in Section 3.3 can be used. However, since there is no tree level FCNC in the left-chiral as well as the right-chiral sector (our choice of $\mathcal{U}_R = \mathbf{1}$ ensures this), the process $t \to c\gamma$ does not receive any contribution from the new quarks. For $Z \to b\overline{b}$, the vertex correction factor of Eq. (34) can be written as

$$\delta_{b\text{-vertex}} = \frac{\alpha}{\pi}\left(|V_{tb}|^2\, F(x_t) + |V_{t'b}|^2\, F(x_{t'})\right). \tag{58}$$

Apart from these processes, one must also consider the constraints coming from the unitarity of the 4×4 CKM matrix, as in Eq. (8).

3.5. VQ-D-D2

Here, as all elements of the fourth row except $V_{t'b'}$ are taken to be zero, the only affected process is $t \to c\gamma$, originating from the contribution of b' at one loop. There are no effects due to t', as FCNC couplings are absent. The contribution to the form factors is, therefore, same as that shown in Section 3.1.

4. Results

Let us now discuss the bounds on the elements of the quark mixing matrix, in the presence of one or more VQs. To be on the conservative side, we take the theoretical uncertainties as well as experimental error margins at 2σ, *i.e.*, 95% confidence level (assuming the uncertainties to be

Gaussian in nature). The benchmark mass for all the VQs is taken to be 2 TeV, just outside the LHC detection limit.

The one-loop $\Delta B = 1$ and 2 processes, namely, $b \to s\gamma$, $B_s \to \mu^+\mu^-$, and B_s - $\overline{B_s}$ mixing, put bounds on V_{ts}, X_{sb} (Eq. (37)), and $\lambda^{t'}_{sb} \equiv V^*_{t's} V_{t'b}$. In view of the importance of QCD corrections, and uncertainties associated with fixing $\mu_{\rm eff}$ for the radiative decay $b \to s\gamma$, we just compare the branching ratios in the VQ model vis-à-vis the SM. This is an approximation on the universality of the higher-order effects for the SM quarks and the VQs, but at least holds for the QCD corrections. Thus, we have

$$\frac{\mathrm{Br}(B \to X_s\gamma)}{\mathrm{Br}(B \to X_s\gamma)_{\rm SM}} = \left(\frac{\left|V^*_{ts} V_{tb}\right|}{\left|V^*_{ts} V_{tb}\right|_{\rm SM}} \right)^2 \left| \frac{C^{(0)\rm eff}_{7\gamma}(\mu)}{C^{(0)\rm eff}_{7\gamma_{\rm SM}}(\mu)} \right|^2 , \tag{59}$$

where $C^{(0)\rm eff}_{7\gamma_{\rm SM}}(\mu)$ is given by Eq. (20). Similarly, to analyse the bound on $V_{t'b}$ from the process $Z \to b\overline{b}$, we take the ratio

$$\frac{R_b}{R_b^{\rm SM}} \approx \frac{1+\delta_b}{1+\delta_b^{\rm SM}} \tag{60}$$

as the dominant contribution from the VQs appears in the vertex correction factor of Eq. (34).

The new mixing matrix elements may contain nontrivial phases. For our analysis, we parametrize

$$X_{sb} = |X_{sb}| \exp(i\theta) , \quad \lambda^{t'}_{sb} = |\lambda^{t'}_{sb}| \exp(i\delta) . \tag{61}$$

For the complex phase, we use the measurement of β_s in the B_s - $\overline{B_s}$ system:

$$M^s_{12} = \left|M^s_{12}\right| \exp(-2i\beta_s) \tag{62}$$

with $\beta_s = (1.1 \pm 1.6) \times 10^{-2}$.

In a similar vein, the bounds on $V_{cb'}$, $V_{tb'}$, and Z_{ct} can be obtained from $t \to c\gamma$. However, this is not yet observed and only an upper limit, orders of magnitude above the SM prediction, exists [31]. Thus, no stringent bounds on these elements can be obtained from $t \to c\gamma$; rather, constraints from unitarity seem more promising.

The SM estimates and experimental numbers for the observables have been listed in Table 5. Note that the SM numbers for $b \to s\gamma$ or $B_s \to \mu^+\mu^-$ involve V_{ts} which, in turn, is obtained from the B_s - $\overline{B_s}$ system. We discuss the bounds on the magnitude and phase of the new mixing matrix elements for different VQ models, and summarise our results in Table 6. For all the VQ types, we generate several models, specified by the new mixing matrix elements, and see if they pass all the experimental constraints. This produces a scatter plot for the allowed parameter space.

4.1. VQ-S-D1

The only constraint comes from Eq. (5), assuming $\mathcal{U} = \mathbf{1}$:

$$|V_{tb'}| \leq 0.30 , \tag{63}$$

which results in a fast decay $b' \to tW$.

Table 5
SM estimates and experimental numbers for several observables with 2σ error margin.

Observables	Measurement	SM Prediction	Reference
R_b	0.21629 ± 0.00132	0.21578 ± 0.00022	[31,48]
$\mathrm{Br}(b \to s\gamma)$	$(3.32 \pm 0.30) \times 10^{-4}$	$(3.36 \pm 0.46) \times 10^{-4}$	[35,36]
$\mathrm{Br}(B_s \to \mu^+\mu^-)$	$(3.0 \pm 0.8) \times 10^{-9}$	$(3.65 \pm 0.46) \times 10^{-9}$	[31,41]
$\mathrm{Br}(t \to c\gamma)$	$< 1.8 \times 10^{-4}$	$\sim 4 \times 10^{-14}$	[31]
$\mathrm{Br}(t \to cZ)$	$< 5 \times 10^{-4}$	$\sim 1 \times 10^{-14}$	[31,49]

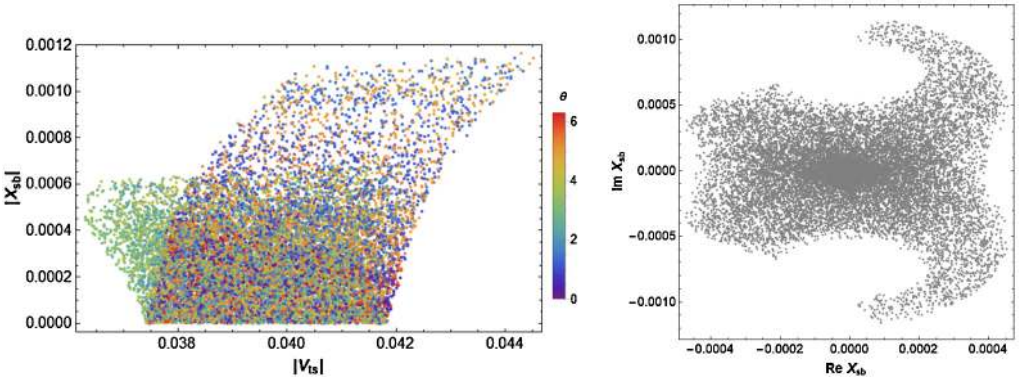

Fig. 1. Constraints from $\Delta B = 1$ and $\Delta B = 2$ processes on $|V_{ts}|$ and X_{sb} for the model VQ-S-D2. (For interpretation of the colours in the figure(s), the reader is referred to the web version of this article.)

4.2. VQ-S-D2

The $\Delta B = 1$ and $\Delta B = 2$ processes put bound on X_{sb} as well as $|V_{ts}|$, which are shown in Fig. 1. Combined constraints from all the three processes, namely, $b \to s\gamma$, $B_s \to \mu^+\mu^-$, and B_s - $\overline{B_s}$ mixing, yield $|X_{sb}| < 1.2 \times 10^{-3}$ and $0.036 < |V_{ts}| < 0.045$. One may note the role the phase θ, associated with X_{sb}, plays in determining the allowed parameter space for both $|X_{sb}|$ and $|V_{ts}|$. On the other hand, constraints from the row unitarity of the 3×4 CKM matrix, Eq. (5), give $|V_{cb'}| \leq 0.15$ and $|V_{tb'}| \leq 0.30$. Using the above bounds, the maximum branching ratio for $t \to c\gamma$ comes out to be $\sim \mathcal{O}(10^{-8})$, still well below the current reach.

4.3. VQ-S-U1

The only process where this model contributes is $Z \to b\bar{b}$, and gives a bound on $V_{t'b}$. The minimum value of $Z_{tt} = |V_{td}|^2 + |V_{ts}|^2 + |V_{tb}|^2$, which is a measure of the deviation from unitarity of the third row of the CKM matrix, comes out to be $Z_{tt} \approx 0.91$. From Eqs. (34), (47), and (60), we obtain $|V_{t'b}| < 0.047$. The column unitarity produces a worse bound: $|V_{t'b}| < 0.30$.

4.4. VQ-S-U2 and VQ-D-U2

Most of the affected processes and the bounds obtained are identical for these two models, so we lump them together. In Fig. 2, we show the bounds on $\lambda^{t'}_{sb}$ and $|V_{ts}|$ arising from B_s - $\overline{B_s}$ mixing, $b \to s\gamma$ and $B_s \to \mu^+\mu^-$. The hollow bell-shaped plot, the right-hand panel of Fig. 2, is

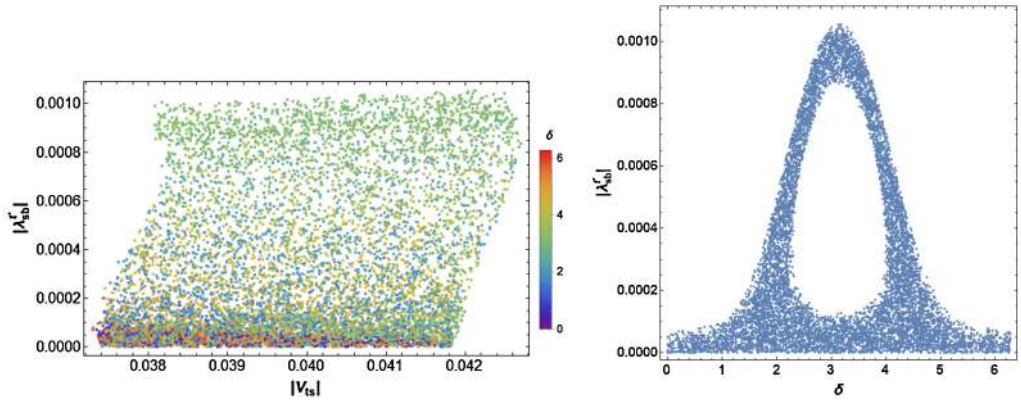

Fig. 2. Constraints from $\Delta B = 1$ and $\Delta B = 2$ processes on $|V_{ts}|$ and $\lambda^{t'}_{sb}$ for the models VQ-S-U2 and VQ-D-U2.

Table 6
Constraints on the quark mixing matrix elements and their combinations in presence of vector-like quarks. A dash indicates that these observables are not affected in the model, whereas entries marked with a dagger indicate that they have been obtained from unitarity constraints. Note that we have taken $V_{t'd}, V_{ub'} = 0$ for all the models.

Model	$\lvert V_{ts}\rvert$	$\lvert X_{sb}\rvert$	$\lvert Z_{ct}\rvert$	$\lvert\lambda^{t'}_{sb}\rvert$	$\lvert V_{t'b}\rvert$	$\lvert V_{cb'}\rvert$	$\lvert V_{tb'}\rvert$
VQ-S-D1	—	0	—	—	—	$\leq 0.15^{\dagger}$	$\leq 0.30^{\dagger}$
VQ-S-D2	0.036 – 0.045	< 0.0012	—	—	—	$\leq 0.15^{\dagger}$	$\leq 0.30^{\dagger}$
VQ-S-U1	—	—	0	0	< 0.047	—	—
VQ-S-U2	0.037 – 0.043	—	< 0.031	< 0.0011	< 0.042	—	—
VQ-D-U2	0.037 – 0.043	—	—	< 0.0011	< 0.045	0	0
VQ-D-D2	—	—	—	0	0	$\leq 0.15^{\dagger}$	$\leq 0.30^{\dagger}$

interesting. Large values of $\lambda^{t'}_{sb}$ near $\delta = \pi$ indicate a destructive interference with the SM, with the VQ amplitude about twice in magnitude compared to the SM one.

Combined constraints from all the three processes give $\left|\lambda^{t'}_{sb}\right| < 1.1 \times 10^{-3}$ and $0.037 < |V_{ts}| < 0.043$. Constraints from the column unitarity of the 4×3 CKM matrix give $|V_{t's}| \leq 0.13$ and $|V_{t'b}| \leq 0.30$. However, one gets a better bound from $Z \to b\bar{b}$, keeping $|V_{t's}| \sim 0.13$: $|V_{t'b}| < 0.042$. This worsens slightly to $|V_{t'b}| < 0.045$ for the VQ-D-U2 model.

From $t \to cZ$ (only for VQ-S-U2), one obtains $|Z_{ct}| < 0.031$. With $|Z_{ct}| \sim \mathcal{O}(10^{-2})$, Br$(t \to c\gamma)$ comes out to be $\sim \mathcal{O}(10^{-8})$. For the texture of the CKM matrix that we have chosen, there is no such FCNC for VQ-D-U2.

4.5. VQ-D-D2

The treatment for the only affected process, namely, $t \to c\gamma$, is identical to that of VQ-S-D2.

A brief summary of our results is displayed in Table 6. We also show, in Table 7, the effect of the VQ mass on these constraints, starting from the present lower bound of 1.5 TeV (approximately) and going up to 10 TeV. Because of the behaviour of the Inami-Lim functions, we find, as expected, that the VQs decouple from the SM (the upper bound on the mixing becomes smaller) with increasing mass.

Table 7
Constraints on the quark mixing matrix elements and their combinations for the VQ mass of 1.5 TeV and 10 TeV. Other constraints are not significantly affected.

	$\lvert\lambda^{t'}_{sb}\rvert$		$\lvert V_{t'b}\rvert$	
$m_{t',b'}$	1.5 TeV	10 TeV	1.5 TeV	10 TeV
VQ-S-U1	0		< 0.062	$< 9.8 \times 10^{-3}$
VQ-S-U2	1.9×10^{-3}	4.4×10^{-5}	< 0.054	$< 9.3 \times 10^{-3}$
VQ-D-U2	1.9×10^{-3}	4.4×10^{-5}	< 0.060	$< 9.1 \times 10^{-3}$

5. Summary

In this paper, we have considered several models with vector-like quarks, including $SU(2)$ singlet and doublet representations, and of charges $+\frac{1}{3}$ and/or $-\frac{2}{3}$, so that they can mix with their SM counterparts. To make our life simple, we assume that they mix only with the third generation quarks, or at the most, with the second and the third generation quarks. This introduces new complex elements in the expanded CKM matrix. At the same time, the 3×3 SM block of the full CKM matrix no longer remains unitary.

We use the low-energy observables, namely, B_s - $\overline{B_s}$ mixing, the decays $b \to s\gamma$ and $B_s \to \mu^+\mu^-$, and the partial decay width R_b, to constrain these new elements. Not all models can be constrained from these observables, and further extensions (like mixing with the first generation quarks) will bring in other observables. Our constraints have been discussed in the previous Section, which are consistent with other similar studies in the literature. We have also found that the width of the anomalous top decay $t \to c\gamma$ may be significantly enhanced in the presence of such VQs, by a few orders of magnitude compared to the SM, but still remains well below the present LHC reach. The parameter space will naturally get more squeezed with new data from LHCb and Belle-II.

Declaration of competing interest

The authors declare that they have no known competing financial interests or personal relationships that could have appeared to influence the work reported in this paper.

Acknowledgements

A.K. acknowledges the support from the Science and Engineering Research Board, Govt. of India, through the grants CRG/2019/000362, MTR/2019/000066, and DIA/2018/000003.

References

[1] H.-J. He, N. Polonsky, S.-f. Su, Extra families, Higgs spectrum and oblique corrections, Phys. Rev. D 64 (2001) 053004, arXiv:hep-ph/0102144.
[2] G.D. Kribs, T. Plehn, M. Spannowsky, T.M. Tait, Four generations and Higgs physics, Phys. Rev. D 76 (2007) 075016, arXiv:0706.3718 [hep-ph].
[3] J. Erler, P. Langacker, Electroweak model and constraints on new physics, arXiv:hep-ph/0407097.
[4] N. Chen, H.-J. He, LHC signatures of two-Higgs-doublets with fourth family, J. High Energy Phys. 04 (2012) 062, arXiv:1202.3072 [hep-ph].
[5] O. Eberhardt, G. Herbert, H. Lacker, A. Lenz, A. Menzel, U. Nierste, M. Wiebusch, Impact of a Higgs boson at a mass of 126 GeV on the standard model with three and four fermion generations, Phys. Rev. Lett. 109 (2012) 241802, arXiv:1209.1101 [hep-ph].

[6] A. Djouadi, A. Lenz, Sealing the fate of a fourth generation of fermions, Phys. Lett. B 715 (2012) 310–314, arXiv:1204.1252 [hep-ph].
[7] E. Kuflik, Y. Nir, T. Volansky, Implications of Higgs searches on the four generation standard model, Phys. Rev. Lett. 110 (9) (2013) 091801, arXiv:1204.1975 [hep-ph].
[8] D. Das, A. Kundu, I. Saha, Higgs data does not rule out a sequential fourth generation with an extended scalar sector, Phys. Rev. D 97 (1) (2018) 011701, arXiv:1707.03000 [hep-ph].
[9] L. Lavoura, J.P. Silva, The Oblique corrections from vector - like singlet and doublet quarks, Phys. Rev. D 47 (1993) 2046–2057.
[10] Y. Okada, L. Panizzi, LHC signatures of vector-like quarks, Adv. High Energy Phys. 2013 (2013) 364936, arXiv:1207.5607 [hep-ph].
[11] H.-J. He, T.M. Tait, C. Yuan, New top flavor models with seesaw mechanism, Phys. Rev. D 62 (2000) 011702, arXiv:hep-ph/9911266.
[12] X.-F. Wang, C. Du, H.-J. He, LHC Higgs signatures from topflavor seesaw mechanism, Phys. Lett. B 723 (2013) 314–323, arXiv:1304.2257 [hep-ph].
[13] H.-J. He, Z.-Z. Xianyu, Extending Higgs inflation with TeV scale new physics, J. Cosmol. Astropart. Phys. 10 (2014) 019, arXiv:1405.7331 [hep-ph].
[14] Y. Liao, X. Li, Nonunitarity of CKM matrix from the vector singlet quark mixing and neutron electric dipole moment, Phys. Lett. B 503 (2001) 301–306, arXiv:hep-ph/0005063.
[15] L. Lavoura, J.P. Silva, Bounds on the mixing of the down type quarks with vector - like singlet quarks, Phys. Rev. D 47 (1993) 1117–1126.
[16] K. Higuchi, K. Yamamoto, Flavor-changing interactions with singlet quarks and their implications for the LHC, Phys. Rev. D 81 (2010) 015009, arXiv:0911.1175 [hep-ph].
[17] D.s. Karabacak, S. Nandi, S.K. Rai, New signal for singlet Higgs and vector-like quarks at the LHC, Phys. Lett. B 737 (2014) 341–345, arXiv:1405.0476 [hep-ph].
[18] C.-H.V. Chang, D. Chang, W.-Y. Keung, Vector quark model and $B \to X_s \gamma$ decay, Phys. Rev. D 61 (2000) 053007.
[19] M. Aoki, E. Asakawa, M. Nagashima, N. Oshimo, A. Sugamoto, Contributions of vector like quarks to radiative B meson decay, Phys. Lett. B 487 (2000) 321–326, arXiv:hep-ph/0005133.
[20] A. Akeroyd, S. Recksiegel, Direct CP asymmetry of $B \to X_{d,s} \gamma$ in a model with vector quarks, Phys. Lett. B 525 (2002) 81–88, arXiv:hep-ph/0109091.
[21] G. Barenboim, F. Botella, $\Delta F = 2$ effective Lagrangian in theories with vector - like fermions, Phys. Lett. B 433 (1998) 385–395, arXiv:hep-ph/9708209.
[22] J. Aguilar-Saavedra, Effects of mixing with quark singlets, Phys. Rev. D 67 (2003) 035003, arXiv:hep-ph/0210112, Erratum: Phys. Rev. D 69 (2004) 099901.
[23] M. Aoki, G.-C. Cho, M. Nagashima, N. Oshimo, Large effects on B_s - $\overline{B_s}$ mixing by vector like quarks, Phys. Rev. D 64 (2001) 117305, arXiv:hep-ph/0102165.
[24] G. Barenboim, F. Botella, O. Vives, Constraining models with vector - like fermions from FCNC in K and B physics, Nucl. Phys. B 613 (2001) 285–305, arXiv:hep-ph/0105306.
[25] T. Morozumi, Z. Xiong, T. Yoshikawa, $B \to X_s l^+ l^-$ and $B \to K\pi$ decays in vector like quark model, arXiv:hep-ph/0408297.
[26] O. Eberhardt, A. Lenz, J. Rohrwild, Less space for a new family of fermions, Phys. Rev. D 82 (2010) 095006, arXiv:1005.3505 [hep-ph].
[27] F. Botella, G. Branco, M. Nebot, The hunt for new physics in the flavour sector with up vector-like quarks, J. High Energy Phys. 12 (2012) 040, arXiv:1207.4440 [hep-ph].
[28] A.K. Alok, S. Banerjee, D. Kumar, S. Uma Sankar, Flavor signatures of isosinglet vector-like down quark model, Nucl. Phys. B 906 (2016) 321–341, arXiv:1402.1023 [hep-ph].
[29] A.K. Alok, S. Banerjee, D. Kumar, S.U. Sankar, D. London, New-physics signals of a model with a vector-singlet up-type quark, Phys. Rev. D 92 (2015) 013002, arXiv:1504.00517 [hep-ph].
[30] A. Denner, S. Dittmaier, A. Muck, G. Passarino, M. Spira, C. Sturm, S. Uccirati, M. Weber, Higgs production and decay with a fourth standard-model-like fermion generation, Eur. Phys. J. C 72 (2012) 1992, arXiv:1111.6395 [hep-ph].
[31] Particle Data Group Collaboration, P.A. Zyla, et al., Review of particle physics, to be published in Prog. Theor. Exp. Phys. 2020 (2020) 083C01.
[32] G. Barenboim, F. Botella, G. Branco, O. Vives, How sensitive to FCNC can B0 CP asymmetries be?, Phys. Lett. B 422 (1998) 277–286, arXiv:hep-ph/9709369.
[33] G. Branco, T. Morozumi, P. Parada, M. Rebelo, CP asymmetries in B0 decays in the presence of flavor changing neutral currents, Phys. Rev. D 48 (1993) 1167–1175.

[34] J. Aguilar-Saavedra, B. Nobre, Rare top decays $t \to c\gamma$, $t \to cg$ and CKM unitarity, Phys. Lett. B 553 (2003) 251–260, arXiv:hep-ph/0210360.
[35] M. Misiak, A. Rehman, M. Steinhauser, NNLO QCD counterterm contributions to $\overline{B} \to X_{s\gamma}$ for the physical value of m_c, Phys. Lett. B 770 (2017) 431–439, arXiv:1702.07674 [hep-ph].
[36] M. Misiak, et al., Updated NNLO QCD predictions for the weak radiative B-meson decays, Phys. Rev. Lett. 114 (22) (2015) 221801, arXiv:1503.01789 [hep-ph].
[37] M. Czakon, P. Fiedler, T. Huber, M. a. Misiak, T. Schutzmeier, M. Steinhauser, The $(Q_7, Q_{1,2})$ contribution to $\overline{B} \to X_s\gamma$ at $\mathcal{O}\left(\alpha_s^2\right)$, J. High Energy Phys. 04 (2015) 168, arXiv:1503.01791 [hep-ph].
[38] SIMBA Collaboration, F.U. Bernlochner, H. Lacker, Z. Ligeti, I.W. Stewart, F.J. Tackmann, K. Tackmann, Precision global determination of the $B \to X_s\gamma$ decay rate, arXiv:2007.04320 [hep-ph].
[39] A.J. Buras, R. Fleischer, Quark mixing, in: CP Violation and Rare Decays After the Top Quark Discovery, vol. 15, 1997, pp. 65–238, arXiv:hep-ph/9704376.
[40] Flavour Lattice Averaging Group Collaboration, S. Aoki, et al., FLAG review 2019: flavour lattice averaging group (FLAG), Eur. Phys. J. C 80 (2) (2020) 113, arXiv:1902.08191 [hep-lat].
[41] C. Bobeth, M. Gorbahn, T. Hermann, M. Misiak, E. Stamou, M. Steinhauser, $B_{s,d} \to l^+l^-$ in the Standard Model with reduced theoretical uncertainty, Phys. Rev. Lett. 112 (2014) 101801, arXiv:1311.0903 [hep-ph].
[42] T. Hermann, M. Misiak, M. Steinhauser, Three-loop QCD corrections to $B_s \to \mu^+\mu^-$, J. High Energy Phys. 12 (2013) 097, arXiv:1311.1347 [hep-ph].
[43] T. Hahn, M. Perez-Victoria, Automatized one loop calculations in four-dimensions and D-dimensions, Comput. Phys. Commun. 118 (1999) 153–165, arXiv:hep-ph/9807565.
[44] G. Eilam, J. Hewett, A. Soni, Rare decays of the top quark in the standard and two Higgs doublet models, Phys. Rev. D 44 (1991) 1473–1484, Erratum: Phys. Rev. D 59 (1999) 039901.
[45] J. Bernabeu, A. Pich, A. Santamaria, Top quark mass from radiative corrections to the $Z \to b\overline{b}$ decay, Nucl. Phys. B 363 (1991) 326–344.
[46] V.D. Barger, M. Berger, R. Phillips, Quark singlets: implications and constraints, Phys. Rev. D 52 (1995) 1663–1683, arXiv:hep-ph/9503204.
[47] P. Bamert, C. Burgess, J.M. Cline, D. London, E. Nardi, R(b) and new physics: a comprehensive analysis, Phys. Rev. D 54 (1996) 4275–4300, arXiv:hep-ph/9602438.
[48] S. Gori, J. Gu, L.-T. Wang, The $Zb\overline{b}$ couplings at future e^+e^- colliders, J. High Energy Phys. 04 (2016) 062, arXiv:1508.07010 [hep-ph].
[49] J. Aguilar-Saavedra, Top flavor-changing neutral interactions: theoretical expectations and experimental detection, Acta Phys. Pol. B 35 (2004) 2695–2710, arXiv:hep-ph/0409342.